 CMES, vol.36, no.1, pp.1-21, 2008

The Shape Identification Problem in Estimating the Geometry of A Three-Dimensional Irregular Internal Cavity

Cheng-Hung Huang[1] **and Chi-An Chen**[1]

Abstract: A three-dimensional shape identification problem (or inverse geometry problem) in estimating the unknown irregular shape of internal cavity by using the steepest descent method (SDM) and a general purpose commercial code CFD-RC is examined in this study based on the simulated measured temperature distributions on the outer surface by infrared thermography. The advantage of calling CFD-RC as a subroutine in the present shape identification problem lies in its characteristics of easily-handling the problem considered here since the auto mesh function of CFD-RC enables the handling of this moving boundary problem.
Three test cases are performed to test the validity and accuracy of the present shape identification algorithm by using different types of cavity shapes, initial guesses and measurement errors. Results show that excellent estimations on the unknown geometry of the internal cavity can be obtained.

1 Nomenclature

$f(x,y,z)$	unknown irregular cavity configuration
J	functional defined by equation (2)
J'	gradient of functional defined by equation (13)
K	thermal conductivity
q_o	heat flux density
S_i	inner surface of cavity
S_o	outer boundary surface
$T(x,y,z)$	estimated temperature
$\Delta T(x,y,z)$	sensitivity function defined by equation (5)
$Y(x,y,z)$	measured temperature

[1] Department of Systems and Naval Mechatronic Engineering, National Cheng Kung University, Tainan, Taiwan, R.O.C.

Greeks

β	search step size defined by equation (7)
Ω	computational domain
$\lambda(x,y,z)$	Lagrange multiplier defined by equation (10)
$\delta(\bullet)$	Dirac delta function
ω	random number
ε	convergence criterion
σ	standard deviation of the measurement errors

Superscript

$\hat{}$	estimated values
n	iteration index

2 Introduction

Recently, shape identification problems or inverse geometry problems have become another area of active research, and many researchers have used infrared scanners in their applications to nondestructive evaluation (NDE) [Hsieh and Su (1980)]. The approaches taken to solve NDE or shape identification problems are based on either steady or unsteady state response of a body subjected to boundary heat fluxes or thermal sources.

For the shape identification problems, it requires a complete regeneration of the mesh as the geometry evolves. Moreover, the continuous evolution of the geometry itself poses certain difficulties in arriving at analytical or numerical solutions. For this reason it is necessary to use an efficient solver such that the above mentioned nature of this problem can be handled, especially for the three-dimensional applications.

The inverse geometry problems, including the cavity or shape estimation, have been solved by a variety of numerical methods [Hsieh and Kassab (1986), Kassab and Hsieh (1987), Hsieh, Choi and Liu (1989), Kassab and Pollard (1994), Dems and Mroz (1987, 1998), Burczinski, Kane, and Balakrishna (1995), Burczynski, Beluch, Dlugosz, Kus, Nowakowski, and Orantek (2002), Cheng and Wu (2000), Aoki, Amaya, Urago, and Nakayama (2005), Forth and Staroselsky (2005) and Mera, Elliott and Ingham (2006)]. Huang and his co-workers have utilized the conjugate gradient method (CGM) and steepest descent method (SDM) to the inverse geometry problems and have published a series of relevant papers.

Huang and Chao (1997) first derived the formulations with CGM in determining the unknown irregular boundary configurations for a two-dimensional, steady-state

shape identification problem. Huang and Tsai (1998) adopted the previous algorithm in Huang and Chao (1997) and extended it to a transient shape identification problem in identifying the unknown irregular boundary configurations from external measurements. Huang, Chiang and Chen (1998) have developed a new algorithm for a two-dimensional multiple cavities estimations where the search directions are not confined in one direction, i.e. the unknown parameters become x- and y-coordinates. Huang and Hsiung (1999) applied the same algorithm in determining the optimal shape of cooling passages for gas turbine. Huang and Chen (1999) extended the similar algorithm to a multiple region domain in estimating the time and space varying outer boundary configurations. Huang and Chaing (2008) applied the technique of SDM to a shape identification problem in estimating the boundary configurations in a three-dimensional domain. In Huang and Chaing (2008) the direction of descent is restricted to only one direction and therefore its algorithm can not be applied to estimate the shape of cavity, unless some modifications are made.

It should be noted that the above references, except for Huang and Chaing (2008), are all the two-dimensional shape identification problems; the three-dimensional shape identification problems are still very limited in the literatures. Recently, Divo, Kassab and Rodriguez (2004) have used a singular superposition technique and the genetic algorithm for detecting the unknown cavity in a three-dimensional inverse geometry problem. In their study the shape of a three-dimensional cavity is only a sphere, not an arbitrary shape, and the convergent speed for the genetic algorithm may also slow.

The objective of this work is to extend the algorithm of previous studies by the authors [Huang and Chao (1997), Huang and Tsai (1998) and Huang and Chaing (2008)] to estimate the unknown three-dimensional shape for internal cavity by utilizing SDM and CFD-RC code (2005) as the subroutine to solve this three-dimensional shape identification problem. The unknown parameters become the x, y and z-coordinates of the cavity and this implies that there is huge number of unknowns in the present study.

The commercial code CFD-RC has the feature of auto mesh and it can be used to calculate many practical but difficult direct thermal problems. If one can devise one algorithm which has the ability to communicate with CFD-RC by means of data communication, a generalized three-dimensional shape identification problem can thus be established.

The SDM is also called an iterative regularization method, which means the regularization procedure is performed during the iterative processes and thus the determination of optimal regularization conditions is not needed. The SDM derives from the perturbation principles and transforms the shape identification problem to

the solution of three problems, namely, the direct, sensitivity and adjoint problems.

These three problems can be solved by CFD-RC and the calculated values are used in SDM for shape identifications. The bridge between CFD-RC and SDM is the INPUT/OUTPUT files. Those files should be arranged such that their format can be recognized by CFD-RC and SDM. A sequence of forward steady-state heat conduction problems is solved by CFD-RC in an effort to update the cavity geometry by minimizing a residual measuring the difference between estimated and measured temperatures at the temperature extracting locations on the outer surface under the present algorithm.

Finally the numerical experiments for this study with three different irregular cavity geometries will be illustrated to show the validity of using SDM in the present three-dimensional shape identification problem.

3 The Direct Problem

To show the methodology for developing expressions for use in determining the unknown internal cavity geometry in a three-dimensional homogeneous medium, the following three-dimensional, steady-state, shape identification problem is considered.

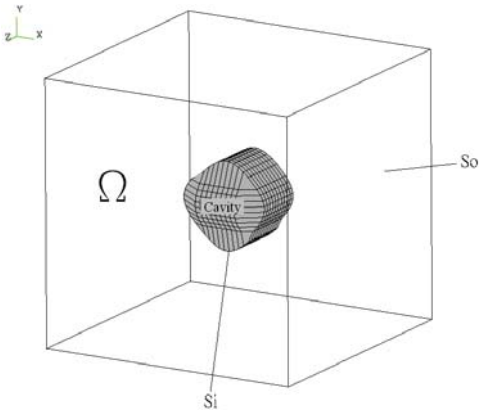

Figure 1: Geometry and coordinates.

For a domain Ω, the boundary condition on inner cavity surface S_i is subjected to the prescribed temperature condition $T = T_i$. The boundary condition on outer boundary surface S_o is subjected to a known heat flux q_o. Figure 1 shows the geometry and the coordinates for the three-dimensional physical problem considered here. The mathematical formulation of this steady-state heat conduction problem

with shape of internal cavity unknown is given by:

$$\frac{\partial^2 T}{\partial^2 x}+\frac{\partial^2 T}{\partial^2 y}+\frac{\partial^2 T}{\partial^2 z}=0 \qquad \text{in } \Omega \tag{1a}$$

$$T=T_i \qquad \text{on inner cavity surface } S_i=f(x,y,z) \tag{1b}$$

$$\pm k\frac{\partial T}{\partial n}=q_o \qquad \text{on outer boundary surface } S_o \tag{1c}$$

here k is the thermal conductivity.

The direct problem considered here is concerned with the determination of the medium temperature when the cavity geometry $f(x,y,z)$ and the boundary conditions at all boundaries are known. The commercial package CFD-RC is used to solve the above direct problem.

4 The Shape Identification Problem

For the shape identification problem, the cavity geometry f(x,y,z) is regarded as being unknown, but everything else in equation (1) is known. In addition, temperature readings taken at some appropriate locations on the outer surface S_o are considered available.

Referring to Figure 1, let the temperature reading taken by an imaginary infrared scanners on the outer surface S_o be denoted by $Y(S_o)\equiv Y(x_m,y_m,z_m)\equiv Y_m(S_o)$, $m=1$ to M, where M represents the number of measured temperature extracting points. It is noted that the measured temperature $Y_m(S_o)$ contain measurement errors. This shape identification problem can be stated as follows: by utilizing the above mentioned measured temperature data $Y_m(S_o)$, estimate the unknown geometry of the internal cavity $f(x,y,z)$.

The solution of the present shape identification problem is to be obtained in such a way that the following functional is minimized:

$$J[f(x,y,z)]=\sum_{m=1}^{M}[T_m(S_0)-Y_m(S_0)]^2 \tag{2}$$

where T_m are the estimated or computed temperatures at the measurement locations (x_m, y_m, z_m) on S_o. These quantities are determined from the solution of the direct problem given previously by using an estimated cavity for the exact $f(x,y,z)$.

5 Steepest Descent Method For Minimization

The steepest descent method (SDM) is similar to but simpler than the conjugate gradient method (CGM) [Alifanov (1994)] since the calculations of the conjugate coefficient and direction of descent are not needed. It is found that SDM can achieve

our goal in the present shape identification study and converges very fast. The following iterative process based on the SDM is now used for the estimation of the unknown shape of cavity $f(x,y,z)$ by minimizing the functional $J[f(x,y,z)]$.

$$f^{n+1}(x^{n+1},y^{n+1},z^{n+1}) = f^n(x^n,y^n,z^n) - \beta^n J'^n \tag{3a}$$

Where

$$J'^n(x,y,z) = J'^n_x \vec{i} + J'^n_y \vec{j} + J'^n_z \vec{k} \tag{3b}$$

or more explicitly

$$x^{n+1} = x^n - \beta^n J'^n_x(x,y,z) \tag{4a}$$

$$y^{n+1} = y^n - \beta^n J'^n_y(x,y,z) \tag{4b}$$

$$z^{n+1} = z^n - \beta^n J'^n_z(x,y,z) \tag{4c}$$

and

$$f^{n+1}(x,y,z) = f(x^{n+1},y^{n+1},z^{n+1}) \tag{4d}$$

Here β^n is the search step size in going from iteration n to iteration $n+1$, $J'^n(x,y,z)$ is the gradient in the outward normal direction while $J'^n_x(x,y,z)$, $J'^n_y(x,y,z)$ and $J'^n_z(x,y,z)$ are the gradients in x, y and z direction, respectively.

To perform the iterations according to equation (3), the step size β^n and the gradients of the functional $J'^n_x(x,y,z)$, $J'^n_y(x,y,z)$ and $J'^n_z(x,y,z)$ need be calculated. In order to develop expressions for the determination of these quantities, a "sensitivity problem" and an "adjoint problem" are constructed as described below.

6 Sensitivity Problem And Search Step Size

The sensitivity problem is obtained from the original direct problem defined by equation (1) in the following manner: It is assumed that when $f(x,y,z)$ undergoes a variation $\Delta f(x,y,z)$, $T(x,y,z)$ is perturbed by $T+\Delta T$. By replacing in the direct problem f by $f+\Delta f$ and T by $T+\Delta T$, subtracting the resulting expressions from the direct problem and neglecting the second-order terms, the following sensitivity problem for the sensitivity function ΔT can be obtained.

$$\frac{\partial^2 T}{\partial^2 x} + \frac{\partial^2 T}{\partial^2 y}\frac{\partial^2 T}{\partial^2 z} = 0 \qquad \text{in } \Omega \tag{5a}$$

$$\Delta T = \Delta f \frac{\partial T}{\partial n} \qquad \text{on inner cavity surface } S_i = f(x,y,z) \tag{5b}$$

$$\frac{\partial \Delta T}{\partial n} = 0 \qquad \text{on outer boundary surface } S_o \tag{5c}$$

where $\frac{\partial T}{\partial n}$ represents the temperature gradient along the normal direction of S_o. The commercial package CFD-RC can be used to solve the above sensitivity problem.

The functional $J(f^{n+1})$ for iteration n+1 is obtained by rewriting equation (2) as

$$J[f^{n+1}] = \sum_{m=1}^{M} \left[T_m(f^n - \beta^n J'^n) - Y_m\right]^2 \tag{6a}$$

where we have replaced f^{n+1} by the expression given by equation (3a). If temperature $T_m(f^n - \beta^n J'^n)$ is linearized by a Taylor expansion, equation (6a) takes the form

$$J(f^{n+1}) = \sum_{m=1}^{M} [T_m(f^n) - \beta^n \Delta T_m(J'^n) - Y_m]^2 \tag{6b}$$

where $T_m(f^n)$ is the solution of the direct problem at (x_m, y_m, z_m) by using estimate shape of cavity for exact f(x,y,z). The sensitivity function $\Delta T_m(J'^n)$ is taken as the solution of problem (5) at the measured positions (x_m, y_m, z_m) by letting $\Delta f = J'^n$. The search step size β^n is determined by minimizing the functional given by equation (6b) with respect to β^n. The following expression results:

$$\beta^n = \frac{\sum_{m=1}^{M} (T_m - Y_m)\Delta T_m}{\sum_{i=m}^{M} (\Delta T_m)^2} \tag{7}$$

7 Adjoint Problem and Gradient Equation

To obtain the adjoint problem, equation (1a) is multiplied by the Lagrange multiplier (or adjoint function) $\lambda(x,y,z)$ and the resulting expression is integrated over the correspondent space domain. The result is then added to the right hand side of equation (2) to yield the following expression for the functional $J[f(x,y,z)]$:

$$\begin{aligned} J[f(x,y,z)] &= \sum_{m=1}^{M} [T_m - Y_m]^2 + \int_{\Omega} \lambda \left(\frac{\partial^2 T}{\partial x^2} + \frac{\partial^2 T}{\partial y^2} + \frac{\partial^2 T}{\partial z^2} \right) d\Omega \\ &= \int_{S_0} [T - Y]^2 \delta(x - x_m)\delta(y - y_m)\delta(z - z_m) dS_0 \\ &\quad + \int_{\Omega} \lambda \left(\frac{\partial^2 T}{\partial x^2} + \frac{\partial^2 T}{\partial y^2} + \frac{\partial^2 T}{\partial z^2} \right) d\Omega \end{aligned} \tag{8}$$

The variation ΔJ is obtained by perturbing f by Δf and T by ΔT in equation (1), subtracting the resulting expression from the original equation (1) and neglecting

the second-order terms. Finally the following expression can be obtained

$$\Delta J = \int_{S_0} 2(T-Y)\Delta T\delta(x-x_m)\delta(y-y_m)\delta(z-z_m)dS_0 + \int_{\Omega} \lambda\left[\frac{\partial^2\Delta T}{\partial x^2}+\frac{\partial^2\Delta T}{\partial y^2}+\frac{\partial^2\Delta T}{\partial z^2}\right]d\Omega \quad (9)$$

where $\delta(\bullet)$ is the Dirac delta function and (x_m, y_m, z_m), $m = 1$ to M, refers to the temperature extracting points for infrared scanners. In equation (9), the domain integral term is reformulated based on Green's second identity; the boundary conditions of the sensitivity problem given by equations (5b) and (5c) are utilized and then ΔJ is allowed to go to zero. The vanishing of the integrands containing ΔT leads to the following adjoint problem for the determination of $\lambda(x,y,z)$:

$$\frac{\partial^2\lambda}{\partial x^2}+\frac{\partial^2\lambda}{\partial y^2}+\frac{\partial^2\lambda}{\partial z^2}=0 \quad (10a)$$

$$\lambda = 0 \text{ on inner cavity surface } S_i = f(x,y,z) \quad (10b)$$

$$\frac{\partial\lambda}{\partial n} = 2(T-Y)\delta(x-x_m)\delta(y-y_m)\delta(z-z_m) \text{ on outer boundary surface } S_o \quad (10c)$$

The commercial package CFD-RC is utilized to solve the above adjoint problem. Finally, the following integral term is left

$$\Delta J = \int_{S_i} -\left[\frac{\partial\lambda}{\partial n}\frac{\partial T}{\partial n}\right]_{\Delta} f(x,y,z)dS_i \quad (11a)$$

From definition [Alifanov (1994)], the functional increment can be presented as

$$\Delta J = \int_{S_i} J'(x,y,z)\Delta f(x,y,z)dS_i \quad (11b)$$

A comparison of equations (11a) and (11b) leads to the following expression for the gradient of functional $J'(x,y,z)$ of the functional $J[f(x,y,z)]$:

$$\begin{aligned} J'(x,y,z) &= -\left.\frac{\partial\lambda}{\partial n}\frac{\partial T}{\partial n}\right|_{S_i} \\ &= -\left(\left.\frac{\partial\lambda}{\partial x}\frac{\partial T}{\partial x}\right|_{S_i}\right)\vec{i} - \left(\left.\frac{\partial\lambda}{\partial y}\frac{\partial T}{\partial y}\right|_{S_i}\right)\vec{j} - \left(\left.\frac{\partial\lambda}{\partial z}\frac{\partial T}{\partial z}\right|_{S_i}\right)\vec{k} \end{aligned} \quad (12)$$

Again, a comparison of equations (3b) and (12) obtain the following gradient equations

$$J'_x(x,y,z) = -\frac{\partial \lambda}{\partial x}\frac{\partial T}{\partial x} \tag{13a}$$

$$J'_y(x,y,z) = -\frac{\partial \lambda}{\partial y}\frac{\partial T}{\partial y} \tag{13b}$$

$$J'_z(x,y,z) = -\frac{\partial \lambda}{\partial z}\frac{\partial T}{\partial z} \tag{13c}$$

The calculation of gradient equation is the most important part of SDM since it plays a significant role of the shape identification calculations.

8 Stopping Criterion

If the problem contains no measurement errors, the traditional check condition specified as follow can be used as the stopping criteria

$$J\left[f^{n+1}(x,y,z)\right] < \varepsilon \tag{14a}$$

where ε is a small specified number and a monotonic convergence can be obtained with SDM. However, the observed temperature data may contain measurement errors. Therefore, it is not expected that the functional equation (2) to be equal to zero at the final iteration step. Following the experience of the author [Alifanov (1994)], the discrepancy principle is used as the stopping criterion, i.e. it is assumed that the temperature residuals may be approximated by

$$T(x_m) - Y(x_m) \approx s \tag{14b}$$

where σ is the standard deviation of the measurement errors, which is assumed to be a constant. Substituting equation (14b) into equation (2), the following expression is obtained for ε:

$$\varepsilon = M\sigma^2 \tag{14c}$$

For this reason the stopping criterion is given by equation (14a) with ε determined from equation (14c).

9 Computational Procedure

The computational procedure for the solution of this shape identification problem using SDM can be summarized as follows:
Suppose $f^n(x,y,z)$ is available at iteration n.

Step 1. Solve the direct problem given by equation (1) for $T(x,y,z)$.

Step 2. Examine the stopping criterion given by equation (14a) with ε given by equation (14c). Continue if not satisfied.

Step 3. Solve the adjoint problem given by equation (10) for $\lambda(x,y,z)$.

Step 4. Compute the gradients of the functional J'_x, J'_y and J'_z from equations (13a), (13b) and (13c), respectively.

Step 5. Set $\Delta f(x,y,z) = J'^n(x,y,z)$, and solve the sensitivity problem given by equation (5) for $\Delta T(x,y,z)$.

Step 6. Compute the search step size β^n from equation (7).

Step 7. Compute the new estimation for $\hat{f}^{n+1}(x,y,z)$ from equation (4) and return to step 1.

10 Results and Discussions

To illustrate the validity of the present inverse geometry problem in identifying irregular configuration of an internal cavity from the knowledge of the simulated temperature recordings taken by an imaginary infrared scanner on the outer surface S_o, three specific examples are considered where the shape of exact and guess cavities are varied.

The geometry of the outer boundary for all the examples considered is taken as a cube with length equal to 10 cm. The thermal conductivity and heat flux are taken as $k = 48W/(m-K)$ and $q_o = -5000$ W/m^2, respectively. The boundary temperature for inner cavity surface is taken as $T_i = 200^o$C.

The objective of this article is to show the accuracy of the present approaches in estimating the inner cavity surface $S_i = f(x,y,z)$, with no prior information on the functional form of the unknown cavity, it is the so-called function estimation.

In order to compare the results for situations involving random measurement errors, the normally distributed uncorrelated errors with zero mean and constant standard deviation were assumed. The simulated inexact measurement data $\mathbf{Y}$ can be expressed as

$$\mathbf{Y} = \mathbf{Y}_{dir} + \omega\sigma \tag{15}$$

where $\mathbf{Y}_{dir}$ is the solution of the direct problem with an exact $f(x,y,z)$; σ is the standard deviation of the measurement error; and ω is a random variable that generated by subroutine DRNNOR of the IMSL (1987) and will be within -2.576 to 2.576 for a 99% confidence bounds.

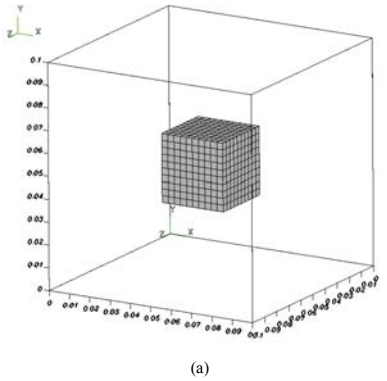

(a)

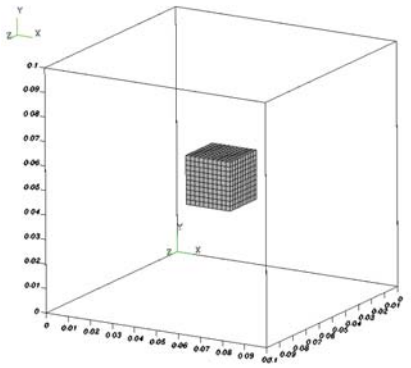

(b)

Figure 2: The (a) type A and (b) type B initial guesses for the shape of internal cavity in the present numerical experiments.

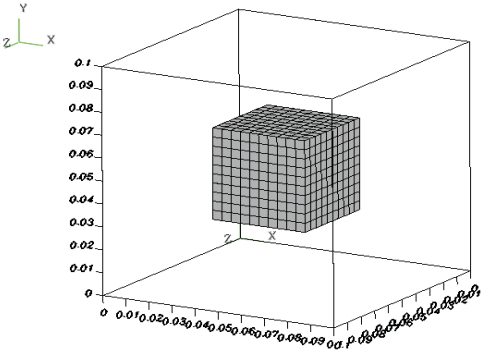

(a)

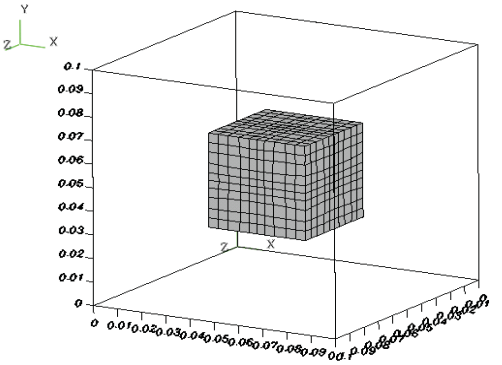

(b)

Figure 3: The (a) exact and (b) estimated cavity configurations with type A initial guess and $\sigma = 0.0$ in case 1.

To examine the effects of different shapes of initial guesses of the cavity to the final estimations, two different shapes of initial guesses are used in this work. The followings define these two types of initial guesses:

Type A: A cube with length equal to 3 cm and its center located at (5,5,5) cm.

Type B: A cube with length equal to 2 cm and its center located at (5,5,5) cm.

the plots for these two initial guesses of the cavity are shown in Figures 2(a) and 2(b), respectively.

One of the advantages of using the SDM is that it does not require a very accurate initial guess of the unknown quantities, this can be verified in the following numerical test cases. However, when there exists a non-physical folding of cavity geometry during the iteration, the inverse calculation must be stopped and used the estimated cavity in the previous step as the initial guess to restart the iteration. We now present below three numerical experiments in estimating the shape of the internal cavity $f(x,y,z)$ by using the SDM.

10.1 Numerical test case 1

The unknown configuration of the exact internal cavity is assumed to be a cube with the center located at (5,5,5) cm and length equal to 4 cm as shown in Figure 3(a). The number of grids used for external and internal domains are both $10\times10\times10$, which implies that each external and internal surface has 121 grid points and therefore there are totally of 602 grid points on the inner cavity surface or (602×3) = 1806 unknown parameters of $x-$, $y-$ and z-coordinates in the present case.

The number of the discreted points for the exact cavity is identical to that for the estimated cavity in the present study and therefore it will not reduce the number of sought-after unknowns. However by applying the discrepancy principle to this shape identification problem will certainly speed up the solution process and regularize the problem to some extent.

First, when assuming exact measurements ($\sigma = 0.0$) and using type A initial guess. By choosing $\varepsilon = 1$, after 168 iterations the estimation can be obtained and the estimated shape of internal cavity by using SDM is shown in Figure 3(b). The measured and estimated temperatures for this case are presented in Figures 4(a) and (b), respectively. The CPU time (on 586-3.0 GHz PC) used in the SDM is about 80 minutes.

The average relative errors for the exact and estimated cavity configurations and for the measured and estimated temperatures are calculated ERR1 = 0.57 % and ERR2 = 0.0074 %, respectively, where the average relative errors ERR1 and ERR2 are defined as

$$\text{ERR1} = \sum_{i=1}^{I} \left| \frac{f(x_i,y_i,z_i) - \hat{f}(x_i,y_i,z_i)}{f(x_i,y_i,z_i)} \right| \div I \times 100\% \tag{16a}$$

$$\text{ERR2} = \sum_{m=1}^{M} \left| \frac{T(x_m,y_m,z_m) - Y(x_m,y_m,z_m)}{Y(x_m,y_m,z_m)} \right| \div M \times 100\% \tag{16b}$$

here $I = M = 602$ represents the total discreted number of grid on the cavity surface and total number of measurements, respectively, while f and $\hat{f}$ denote the exact and estimated values of cavity configurations, respectively. It can be seen from

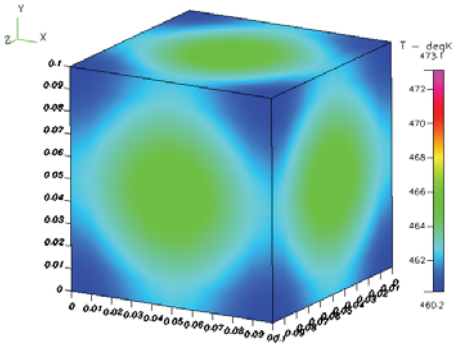

(a)

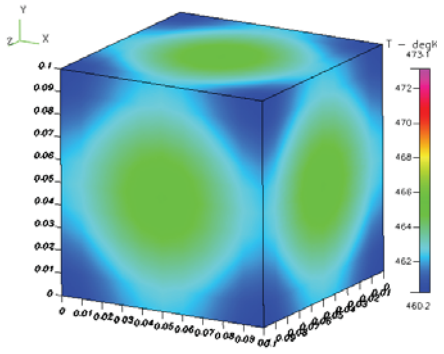

(b)

Figure 4: The (a) measured and (b) estimated surface temperatures on S_o with $\sigma = 0.0$ in case 1.

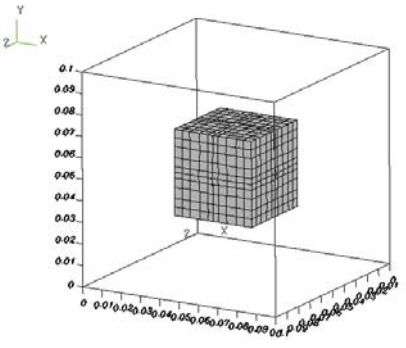

(a)

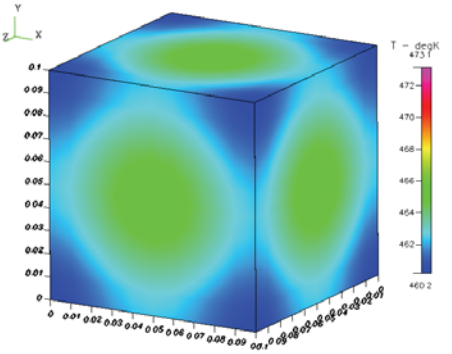

(b)

Figure 5: The (a) estimated cavity using type B initial guess and (b) estimated surface temperatures on S_o with $\sigma = 0.0$ in case 1.

the above figures and relative average errors that the present shape identification scheme obtained good estimation for $f(x,y,z)$ since the sharp corner of cube can still be reconstructed without assuming any extra conditions.

Next, it would be of interest to examine what will be happen when different initial guess is considered. The computational conditions are the same as the previous case except that type B initial guess is now chosen.

By choosing $\varepsilon = 1$ and $\sigma = 0.0$, after 39 iterations the estimated shape of internal cavity is shown in Figure 5(a). The estimated temperatures for this case are presented in Figure 5(b). The relative average errors ERR1 and ERR2 are calculated as ERR1 = 0.63 % and ERR2 = 0.0066 %. Again, it can be seen from these Figures

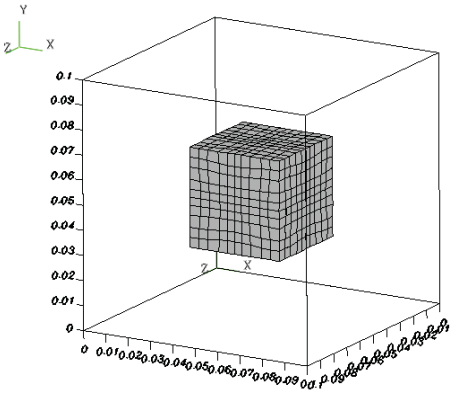

(a)

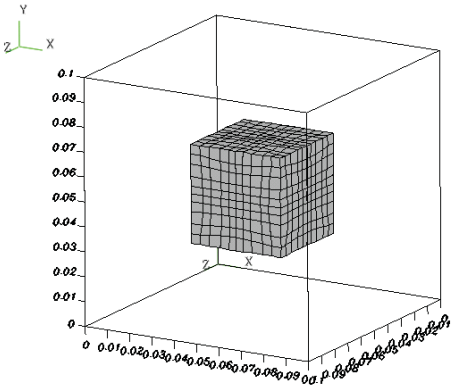

(b)

Figure 6: The estimated internal cavity by using (a) σ = 0.3 and (b) σ = 0.42 and type A initial guess in case 1.

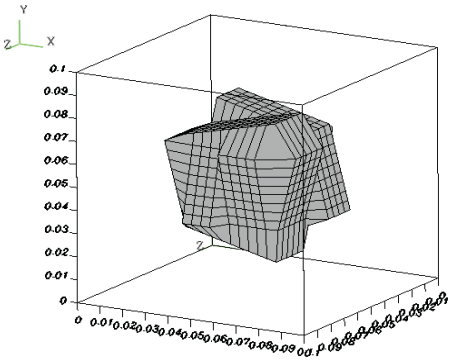

(a)

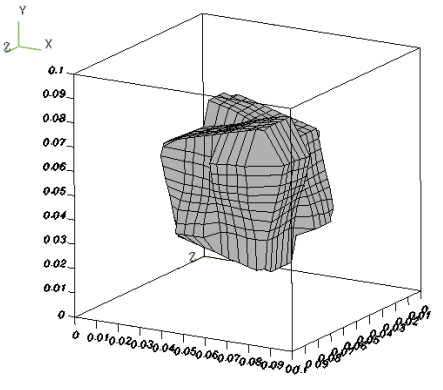

(b)

Figure 7: The (a) exact and (b) estimated cavity configurations with type A initial guess and σ = 0.0 in case 2.

and data that this algorithm obtained good estimation of $f(x,y,z)$, especial for the sharp corner, even though the initial guess is different.

Finally, the influence of the measurement errors on the shape identification problems needs to be discussed. First, the measurement error for the simulated temperatures measured by imaginary infrared scanner on outer surface S_o is taken as σ = 0.3 (about 5 % of the largest temperature difference on S_o). The estimations for f(x,y,z) can be obtained after only 87 iterations and plotted in Figures 6(a). The relative average errors ERR1 and ERR2 are calculated as ERR1 = 0.81 % and ERR2 = 0.053 %, respectively.

The measurement error for the temperatures is then increased to $\sigma = 0.42$ (about 7 % of the largest temperature difference on S_o). After only 64 iterations the estimated $f(x, y, z)$ are obtained and illustrated in Figures 6(b). ERR1 and ERR2 are calculated as 0.95 % and 0.074 %, respectively.

From Figures 3 to 6 we have learned that as the measurement errors are increased the accuracy of the estimated cavity shape is decreased, however, they are still reliable. Therefore the present technique provides confidence estimation.

10.2 Numerical test case 2

In order to show the ability in handling more irregular shape for the internal cavity, in the second test case we consider an exact cavity domain as shown in Figure 7(a). The computational conditions are the same as used in numerical test case 1 and type A initial guess for the cavity is used.

When assuming exact measurements $\sigma = 0.0$, and $\varepsilon = 3.0$, after 23 iterations, the estimated shape of internal cavity by using SDM is shown in Figure 7(b). The measured and estimated temperatures for this case are presented in Figures 8(a) and 8(b), respectively.

The average relative errors for the exact and estimated cavity configurations and for the measured and estimated temperatures are calculated ERR1 = 0.90 % and ERR2 = 0.011 %, respectively. It is clear from the above figures, ERR1 and ERR2 that good estimation for f(x,y,z) can be obtained by the present shape identification scheme.

Finally, let us examine the influence of the measurement errors on the shape identification problems. First, the measurement error for the simulated temperatures measured by imaginary infrared scanner on outer surface S_o is taken as $\sigma = 0.28$ (about 5 % of the largest temperature difference on S_o), then it is increased to $\sigma = 0.39$ (about 7 % of the largest temperature difference on S_o). The estimations for $f(x, y, z)$ can be obtained after 18 and 16 iterations, respectively and the results for the estimated cavities are plotted in Figures 9(a) and 9(b), respectively. The relative average errors for $\sigma = 0.28$ are calculated as ERR1 = 0.97 % and ERR2 = 0.049 % and for $\sigma = 0.39$ are calculated as ERR1 = 0.95 % and ERR2 = 0.069 %. Again, the present technique provides confidence estimation.

10.3 Numerical test case 3

To test the ability of this algorithm, in the third test case we considered another irregular shape as the exact cavity domain which is shown in Figure 10(a). It can be seen from Figure 10(a) that there exist many step surfaces on S_0 and this make the estimation more difficult. Type A initial guess is used in test case 3 and the

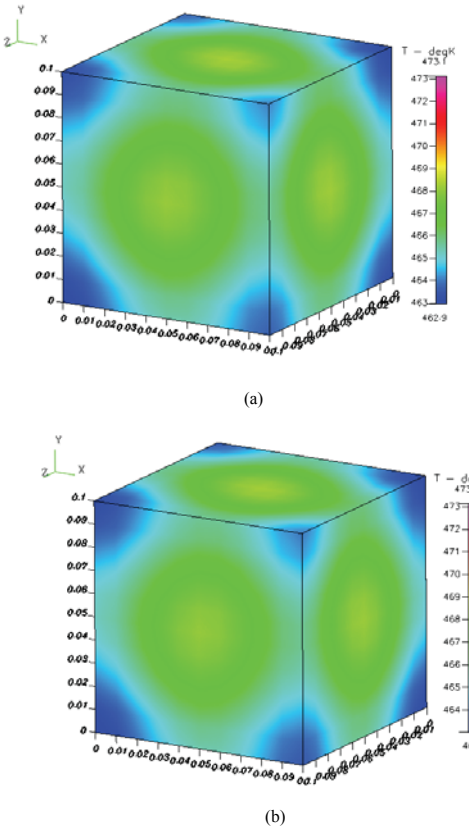

Figure 8: The (a) measured and (b) estimated surface temperatures on S_o with σ = 0.0 in case 2.

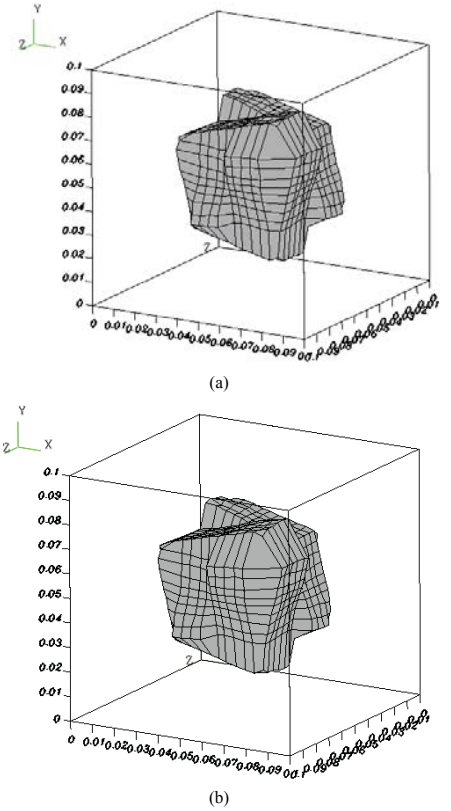

Figure 9: The estimated internal cavity by using (a) σ = 0.28 and (b) σ = 0.39 and type A initial guess in case 2.

computational conditions are the same as used in numerical test case 2.

When assuming exact measurements $\sigma = 0.0$ and $\varepsilon = 5.0$, and after 1520 iterations, the estimated shape of internal cavity by using SDM is shown in Figure 10(b). The measured and estimated temperatures for this case are presented in Figures 11(a) and 11(b), respectively.

The average relative errors for the exact and estimated cavity configurations and for the measured and estimated temperatures are calculated ERR1 = 0.78 % and ERR2 = 0.024 %, respectively. The reason for needing this huge number of iterations is because that to match with the sharp corner for the step functions on S_o, the estimated coordinates must be very accurate otherwise the shape of internal irregular cavity can not be reconstructed accurately. It is clear from the above figures, ERR1 and ERR2 that good estimation for $f(x,y,z)$ can be obtained by the present shape identification scheme.

Finally, the measurement error for the simulated temperatures measured by imaginary infrared scanner on outer surface S_o is taken as $\sigma = 0.3$ (about 5 % of the largest temperature difference on S_o). The estimations for $f(x,y,z)$ can be obtained after 292 iterations and the results for the estimated cavities are plotted in Figure 12(a). The relative average errors are calculated as ERR1 = 0.818 % and ERR2 = 0.054 % .

Next, the measurement error is increased to $\sigma = 0.42$ (about 7 % of the largest temperature difference on S_o). The estimation for cavity is obtained after 175 iterations and the results for the estimated cavities are shown in Figure 12(b). The relative average errors are obtained as ERR1 = 0.946 % and ERR2 = 0.076 %, respectively.

From the above three numerical test cases, it is learned that the SDM in estimating unknown internal cavity does not need any assumptions such as the cubic spline fitting used in Kassab and Pollard (1994). When unknown cavities have some "sharp" corners such as the shape of a step function, the SDM can still be applied to obtain good estimation but a cubic spline APG algorithm may not perform well since cubic spline fitting can not produce any sharp corners.

11 Conclusions

The steepest descent method (SDM) together with the commercial code CFD-RC were successfully applied for the solution of the three dimensional inverse geometry problem to determine the unknown three-dimensional irregular cavity configurations by utilizing surface temperature readings. Three test cases involving different shape of exact cavity, different shape of initial guess cavity and different measurement errors were considered. The results show that the SDM does not re-

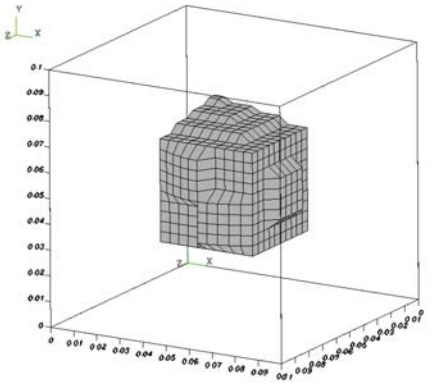

(a)

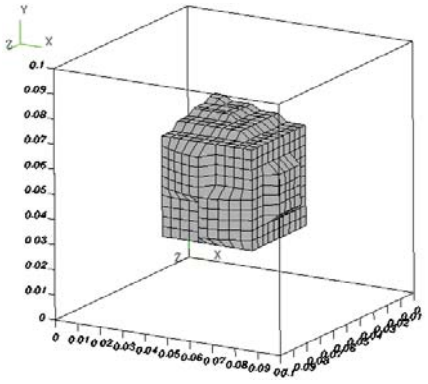

(b)

Figure 10: The (a) exact and (b) estimated cavity configurations with type A initial guess and σ = 0.0 in case 3.

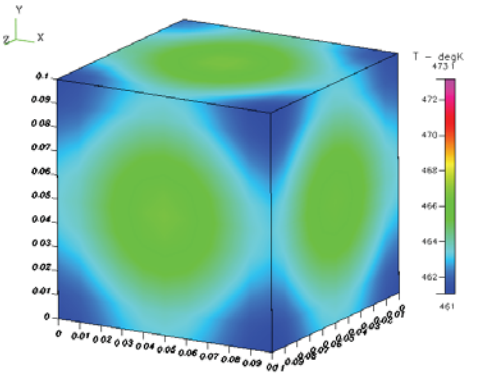

(a)

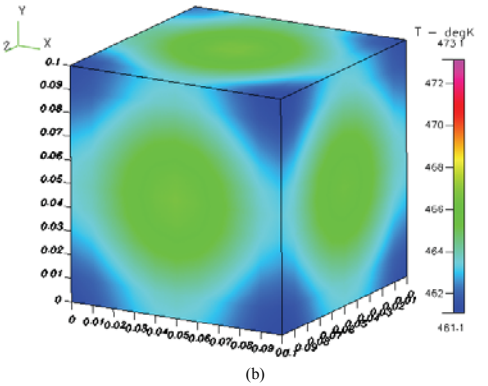

(b)

Figure 11: The (a) measured and (b) estimated surface temperatures on S_o with σ = 0.0 in case 3.

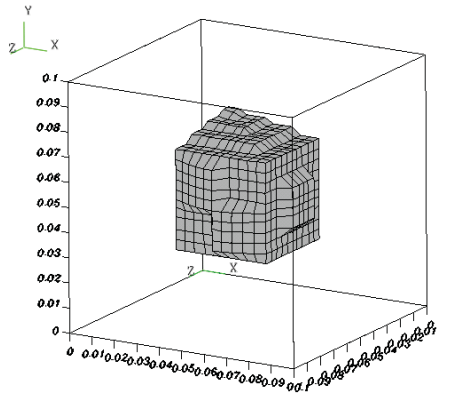

(a)

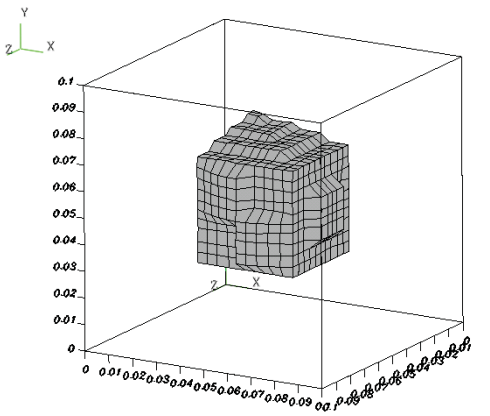

(b)

Figure 12: The estimated internal cavity by using (a) $\sigma = 0.3$ and (b) $\sigma = 0.42$ and type A initial guess in case 3.

quire an accurate initial guesses of the unknown quantities, does not need any extra assumptions such as cubic spline fitting used in Kassab and Pollard (1994), needs short CPU time on 586-3.0 GHz PC and is not sensitive to the measurement errors when performing the shape identifying calculations.

Acknowledgement: This work was supported in part through the National Science Council, R. O. C., Grant number, NSC-96-2221-E-006-065.

12 References

Alifanov, O. M. (1994): *Inverse heat transfer problems*. Springer-Verlag, Berlin Heidelberg.

Aoki, S.; Amaya, K.; Urago, M.; Nakayama, A. (2005): Fast Multipole Boundary Element Analysis of Corrosion Problems. *CMES: Computer Modeling in Engineering & Sciences*, vol. 6, no. 2, pp. 123–132.

Burczynski, T., Beluch, W., Dlugosz, A., Kus, W., Nowakowski, M., Orantek, P. (2002): Evolutionary Computation in Optimization and Identification, *Comput. Assist. Mech. Eng. Sci.,* Vol. 9, pp. 3–20.

Burczinski,T., Kane, J. H., Balakrishna, C. (1995): Shape Design Sensitivity Analysis via Material Derivative-Adjoint Variable Technique for 3D and 2D Curved Boundary Elements, *Int. J. Numer. Meth. Eng.,* Vol. 38, pp. 2839–2866.

CFD-RC user's manual, ESI-CFD Inc. (2005).

Cheng, C. H., Wu, C. Y. (2000): An Approach Combining Body-Fitted Grid Generation and Conjugate Gradient Methods for Shape Design in Heat Conduction Problems, *Numer. Heat Transfer B,* Vol. 37, pp. 69–83.

Dems, K., Mroz, Z. (1987): Variational approach to sensitivity analysis in thermoelasticity, *J. Thermal Stresses,* Vol. 10, pp.283–306.

Dems, K., Mroz , Z. (1998): Sensitivity analysis and optimal design of external boundaries and interfaces for heat conduction systems , *J. Thermal Stress,* Vol. 21, No. 3-4, pp. 461-488.

Divo, E., Kassab, A. J., Rodriguez, F. (2004): An Efficient Singular Superposition Technique for Cavity Detection and Shape Optimization, *Numerical Heat Transfer,* Part B, Vol. 46, pp. 1-30.

Forth, S.; Staroselsky, A. (2005): A Hybrid FEM/BEM Approach for Designing an Aircraft Engine Structural Health Monitoring. *CMES: Computer Modeling in Engineering & Sciences*, vol. 9, no. 3, pp. 287–298.

Hsieh, C. K., Choi, C. Y., Liu, K. M. (1989): A Domain Extension Method for Quantitative Detection of Cavities by Infrared Scanning, *J. Nodes. Eval.*, Vol. 8, pp. 195-211.

Hsieh, C. K., Kassab, A. J. (1986): A General Method for the Solution of Inverse Heat Conduction Problems with Partially Specified System Geometries, *Int. J. Heat Mass Transfer,* Vol. 29, pp. 47-58.

Hsieh, C. K., Su, K. C. (1980): A Methodology of Predicting Cavity Geometry Based on the Scanned Surface Temperature Data-Prescribed Surface Temperature at the Cavity Side, *J. Heat Transfer*, Vol. 102, No. 2, pp. 324-329.

Huang, C. H., Chaing, M. T. (2008): A Transient Three-Dimensional Inverse Geometry Problem in Estimating the Space and Time-Dependent Irregular Boundary Shapes, *Int. J. Heat and Mass Transfer.* Vol. 51, No. 21-22, pp. 5238–5246.

Huang, C. H., Chao, B. H. (1997): An Inverse Geometry Problem in Identifying Irregular Boundary Configurations, *Int. J. Heat and Mass Transfer*, Vol. 40, pp. 2045-2053.

Huang, C. H., Chen, H. M. (1999): An Inverse Geometry Problem of Identifying Growth of Boundary Shapes in A Multiple Region Domain, *Numerical Heat Transfer*; Part A, Vol. 35, pp. 435-450.

Huang, C. H., Chiang, C. C., Chen, H. M. (1998): Shape Identification Problem in Estimating the Geometry of Multiple Cavities, *AIAA, J. Thermophysics and Heat Transfer*, Vol. 12, pp. 270-277.

Huang, C. H., Hsiung, T. Y. (1999): An Inverse Design Problem of Estimating Optimal Shape of Cooling Passages in Turbine Blades, *Int. J. Heat and Mass Transfer*, Vol. 42, No. 23, pp. 4307-4319.

Huang, C. H., Tsai, C. C. (1998): A Transient Inverse Two-Dimensional Geometry Problem in Estimating Time-Dependent Irregular Boundary Configurations, *Int. J. Heat and Mass Transfer*, Vol. 41, pp. 1707-1718.

IMSL Library Edition 10.0 (1987): User's Manual: Math Library Version 1.0, IMSL, Houston, TX.

Kassab, A. J., Hsieh, C. K. (1987): Application and Infrared Scanners and Inverse Heat Conduction Methods to Infrared Computerized Axial Tomography, *Rev. Sci. Inst.,* Vol. 58, pp. 89-95.

Kassab, A. J., Pollard, J. (1994): A Cubic Spline Anchored Grid Pattern Algorithm for High Resolution Detection of Subsurface Cavities by the IR-CAT Method, *Num. Heat Transfer*, Part B, Vol. 26, pp. 63-78.

Mera, N. S., Elliott, L., Ingham, D. B. (2006): The Detection of Super-elliptical Inclusions in Infrared Computerised Axial Tomography, *CMES: Computer Modeling in Engineering & Sciences*, Vol. 6, No. 2, pp. 123-132.